



UNIVERSITY OF LEEDS

This is a repository copy of *An efficient plasmonic photovoltaic structure using silicon strip-loaded geometry*.

White Rose Research Online URL for this paper:  
<http://eprints.whiterose.ac.uk/110325/>

Version: Accepted Version

---

**Article:**

Awal, MA, Ahmed, Z and Talukder, MA [orcid.org/0000-0002-2814-3658](http://orcid.org/0000-0002-2814-3658) (2015) An efficient plasmonic photovoltaic structure using silicon strip-loaded geometry. *Journal of Applied Physics*, 117 (6). 063109. ISSN 0021-8979

<https://doi.org/10.1063/1.4907873>

---

© 2015, AIP Publishing LLC. This article may be downloaded for personal use only. Any other use requires prior permission of the author and AIP Publishing. The following article appeared in *Journal of Applied Physics* and may be found at <http://dx.doi.org/10.1063/1.4907873>

**Reuse**

Unless indicated otherwise, fulltext items are protected by copyright with all rights reserved. The copyright exception in section 29 of the Copyright, Designs and Patents Act 1988 allows the making of a single copy solely for the purpose of non-commercial research or private study within the limits of fair dealing. The publisher or other rights-holder may allow further reproduction and re-use of this version - refer to the White Rose Research Online record for this item. Where records identify the publisher as the copyright holder, users can verify any specific terms of use on the publisher's website.

**Takedown**

If you consider content in White Rose Research Online to be in breach of UK law, please notify us by emailing [eprints@whiterose.ac.uk](mailto:eprints@whiterose.ac.uk) including the URL of the record and the reason for the withdrawal request.



[eprints@whiterose.ac.uk](mailto:eprints@whiterose.ac.uk)  
<https://eprints.whiterose.ac.uk/>

# An efficient plasmonic photovoltaic structure using silicon strip-loaded geometry

M A Awal,<sup>1</sup> Zabir Ahmed,<sup>1</sup> and Muhammad Anisuzzaman Talukder<sup>1,2</sup>

<sup>1</sup>Department of Electrical and Electronic Engineering

Bangladesh University of Engineering and Technology

Dhaka 1205, Bangladesh

<sup>2</sup>Department of Computer Science and Electrical Engineering

University of Maryland, Baltimore County

1000 Hilltop Circle, Baltimore, MD 21250, USA

anis@eee.buet.ac.bd

## Abstract

We show that a silicon thin-film photovoltaic structure with silicon strips on the top and grooves on the silver back contact layer can absorb incident solar energy over a broad spectral range. The silicon strips on the top scatter the incident light and significantly help couple to the photonic modes in the smaller wavelength range. The grooves on the silver back contact layer both scatter the incident light and help couple to the photonic modes and resonant surface plasmon polaritons. We find an increase of  $\sim 46\%$  in total integrated solar absorption in

the proposed strip-loaded structure compared to that in a planar thin film structure of same dimensions. The proposed structure offers simpler fabrication compared to similar plasmonic-inspired designs.

## 1 Introduction

Light confinement in photovoltaic structures of sub-wavelength dimensions is of significant interest as it may be a key to improving efficiency to cost ratio in solar cells. Sub-wavelength plasmonic structures are being investigated for increased light confinement, since, in principle, plasmonic structures can confine light beyond the diffraction limit [1, 2]. Increased light confinement is possible through excitation of surface plasmon polaritons (SPPs) in corrugated dielectric/metal interfaces and localized surface plasmons in metal nano-particles embedded in dielectric material of sub-wavelength dimensions [3–8]. However, plasmonic resonances due to surface plasmon polaritons are much stronger in the longer wavelength range of the available solar spectrum. By contrast, in a silicon (Si) solar cell, absorption is much stronger in the smaller wavelength range. Therefore, even with a strong plasmonic resonance in a photovoltaic structure, the total integrated absorption of solar spectrum due to plasmonic resonance is usually not significant.

In order to maximize the total integrated absorption, incident solar energy also has to be confined in the form of waveguide modes, which are also called photonic modes. Photonic modes can be excited without a metal structure and are not bound to a surface, rather spread throughout the active region. Therefore, light coupled to the photonic modes not only reduces loss in metal but also increases carrier collection efficiency. By contrast, light coupled to plasmonic modes enhances field in the proximity of the metal body, which results non-uniform photo-carrier generation, and

thus, a reduced carrier collection efficiency.

A number of techniques have been investigated to excite photonic modes in solar cells, the simplest of which might be the periodic texturing of metal back contact [8]. The photonic modes excited in SPP-inspired designs with period texturing of metal back contact provide a very limited scope for optimization as SPP modes also have to be optimized simultaneously. However, plasmonic structures with metal strips on silica-coated thin film Si supported on silica substrate has been shown to help excite and optimize photonic modes [9]. Though such a structure shows  $\sim 43\%$  enhancement in short circuit current gain compared to a structure without metal strips, the sophistication of the design makes it significantly difficult to fabricate even with the state of the art process technologies. Recently, a more complex structure using 2D silver (Ag) grating on top surface has been reported to produce broadband absorption [10]. It has been shown that by controlling the 2D grating parameters, incident light can be coupled to multiple resonant localized surface plasmon and resonant photonic modes. However, precise control over the 2D Ag grating width and period of the cascaded structure is essential for resonant broadband absorption, which will be immensely difficult to fabricate.

Light absorption in surface plasmon-inspired thin film solar cells can also be increased by transferring the incident solar energy between discrete metal nano-particles to excite modes spreading throughout the structure [11]. This technique achieves a significant absorption enhancement even without a reflective back contact, but impact of relative positions of discrete metal nano-particles and accuracy of dimensions make it quite difficult to fabricate. Additionally, photonic crystal based back reflectors have been shown to increase light absorption up to 50% in solar cells [12–17]. All these techniques improve solar cell performance to some extent at the expense of significant additional fabrication costs and difficulties.

There are various fabrication techniques for depositing periodic and random shapes on already fabricated solar cells [18]. However, it is difficult to pattern metal nano-particles with precision on solar cell structures due to aggregation [19]. By contrast, fabrication is relatively easier for corrugated metal back contacts [20]. Nano-imprint lithography is usually used for corrugated metal back contact fabrication as this technique offers capacity in large area processing and precise control of the nano-structures [21, 22]. Considering the costs and complexities related to the fabrication of many earlier proposals, this work aims at designing an efficient structure with cheaper and simpler fabrication possibility.

In this work, we design a silicon thin-film solar cell for broadband light absorption with silicon strip-loaded geometry on the top and periodic corrugation on the metal back contact. The silicon strips on the top help the incident light to scatter and thus couple into the photonic modes within the active region. The periodic corrugation on the back contact helps excite the SPPs. Photonic modes contribute to the absorption in the shorter wavelength range, while SPPs contribute to the absorption in the longer wavelength range of the available solar spectrum. A detailed investigation of the designed structure shows that the total integrated absorption weighted by the available solar spectrum increases by 45.7% compared to that in a plain silicon slab structure.

## **2 Proposed Structure**

The proposed structure is schematically shown in Fig. 1(a). In the proposed structure, the silicon active layer is bound by two silica spacer layers on top and bottom. In the top spacer, part of the silica layer is replaced by silicon strips in a periodic fashion. This design is based on strip-loaded waveguide theory [23]. The silicon strips in the silica spacer layer make the effective index of

the silicon active region beneath the strip greater than the actual material index. Therefore, the active region, though not surrounded by materials of smaller index, effectively forms a waveguide with confinement in both  $x$ - and  $y$ -directions. The silicon strips on top surface scatter the incident light to couple to the photonic modes. In the proposed structure, we use silicon strips instead of metal strips as has been proposed on the spacer layer in Ref. [9]. The use of silicon strips reduces the back scattering of the incident light, which happens if the metal strips are used. The use of silicon strips instead of metal strips also makes the structure cheaper and simpler to fabricate. The proposed structure has periodic rectangular grooves at the dielectric-metal back contact. The metal back contact with grooves will help excite SPPs at longer wavelength and thus confine light in that range as well as couple shorter wavelength light to photonic modes.

In this work, we design and optimize a silicon strip-loaded solar cell with a single layer of crystalline silicon as the active region. We present our analysis with crystalline silicon active region as it is the mostly used solar cell material at this time. Additionally, crystalline silicon has a carrier diffusion length of  $\sim 100 \mu\text{m}$ , which is much greater than the  $\sim 100 \text{ nm}$  carrier diffusion length of amorphous (a-Si) or nanocrystalline silicon [24,25]. Therefore, all the carriers generated in a crystalline silicon active layer of sub-wavelength dimension can be fairly approximated to be collected at the contact terminals, so that a detailed light absorption calculation gives an accurate understanding of the short-circuit current density. However, since the increased light absorption in the proposed strip-loaded structure is mainly due to the spatial index contrast created in the longitudinal direction, other solar cell materials such as amorphous silicon and nanocrystalline silicon can be used as the active region for increased light absorption. Additionally, multiple layers as in tandem solar cells can also be used as the active region. In particular, we present absorption profiles for amorphous silicon active regions in addition to the crystalline silicon active regions.

We note that when the proposed strip-loaded structure is used for practical solar cells, the top surfaces of the silicon strips have to be oxidized to collect current from the strips. Additionally, there will be anti-reflection indium tin oxide (ITO) layer on the top of the proposed structure to reduce the reflection of the incident solar energy from the top surface of the solar cells. Although ITO layer increases overall light coupling to the solar cell, a fraction of the coupled light gets trapped within ITO layer due to excitation of resonant Fabry-Perot modes. [15–17]. However, in any case, the behavior of the proposed strip-loaded structure to the light that is transmitted through the oxide layer and incident on the active region will be similar.

### 3 Simulation Approach

To investigate the response of the proposed structure to the incident light, we solve Maxwell’s electromagnetic equations using full-field finite difference time domain (FDTD) technique. We find the solutions for two dimensional structures as the proposed structure is invariant in the  $z$ -direction. In our simulation setup, as shown in Fig. 1(b), we apply periodic boundary conditions in the  $y$ -direction and perfectly matched layers (PMLs) in the  $x$ -direction.

In this work, we study the response of the proposed structure to both transverse magnetic (TM) and transverse electric (TE) plane polarized and normally incident light. The incident light is a broadband pulse that covers the available solar energy on earth between 400 nm to 1000 nm range. After we solve the steady-state response, we calculate the absorption at a point by  $\frac{1}{2} \times \omega \times \text{Im}(\epsilon) |\vec{E}|^2$ , where  $\vec{E}$  is the steady-state electric field,  $\omega$  is the frequency of the incident light, and  $\epsilon$  is the permittivity of the material [26]. The total absorption in silicon and metal layer is calculated by integrating this expression over the entire layer. We find the normalized absorption

by calculating the ratio of absorbed energy to incident energy. Since the solar irradiation varies with wavelength as shown in Fig. 2, finally, we normalize absorption in a layer by the solar spectral irradiance distribution.

## 4 Analysis

### 4.1 Resonant modes

The response of the proposed structure depends on the wavelength and the polarization of the incident light. Depending on the wavelength, the incident light can couple to resonant Fabry-Perot modes, photonic modes or plasmonic modes. In Fig. 3, we show examples when strong Fabry-Perot modes and photonic modes are created for TE and TM incident light. In Fig. 3(a), we show strong Fabry-Perot modes for TE incident light at a wavelength of 900 nm. In Fig. 3(b), we show strong Fabry-Perot modes for TM incident light at a wavelength of 780 nm. However, for TM incident light, we note that the Fabry-Perot modes are somewhat distorted. The distortion is due to the interaction between the Fabry-Perot modes and the resonant SPPs created at the back metal-dielectric interface. In Fig. 3(c), we note two dimensional confinements, which are resonant photonic modes for TE incident light at 820 nm. Similarly, in Fig. 3(d), we note two dimensional confinements, which are resonant modes for TM incident light at 800 nm. These resonant photonic modes are created mainly due to the scattering of the incident light by silicon strips on the top.

## 4.2 Absorption profiles

In Fig. 4, we show the overall absorption profiles in the silicon active layer and silver layer of the proposed silicon strip-loaded structure when the incident light is TM polarized. In Fig. 4, we also show absorption profiles of a planar structure where the silicon active layer is bound by two silica spacer layers and of a structure where the top silica layer is periodically replaced by silver strips instead of silicon strips of the proposed structure.

We note that the absorption profile in a planar structure is dominated by Fabry-Perot resonances. In the absorption profile of the proposed structure, there are a number of peaks in addition to the Fabry-Perot resonances. These peaks are due to resonant photonic and plasmonic modes. The photonic modes result in absorption peaks only in silicon but not in metal and these modes are prominent in the shorter wavelength regime of the available solar spectrum. These modes are caused by the two dimensional confinement imposed by the strip loaded geometry. In addition to the transverse confinement due to the silicon strips, the symmetry of the active silicon layer with silica spacer on both sides supports both the even and odd modes in the longitudinal direction. By contrast, the surface plasmon resonances are easily distinguished by absorption peaks in silicon in the longer wavelength range with corresponding absorption peaks in metal back contact layer. If metal strips replace the silicon strips, photonic modes are created too. However, the absorption in the active silicon layer decreases due to a huge loss in the metal strips and reflection of the incident light by the metal strips. In Fig. 4(b), we note that the absorption in Ag layer of the structure with Ag strips is much greater than that of the structure with Si strips. We also note that the absorption in silicon layer of the structure with Ag strips significantly decreases in the blue part of the spectrum, which is mainly due to the Fano resonance in the Ag strips at this spectrum range [8].

In Fig. 5, overall absorption profiles are given in the silicon and metal layers of the same three photovoltaic structures as in Fig. 4, except that the incident light is TE polarized. The planar structure shows the similar response as with the TM polarized light. However, absorption peaks due to surface plasmon resonances are absent for the proposed structure. We note absorption peaks that are due to resonant photonic modes. However, absorption due to resonant photonic modes decreases with TE incident light. In the structure with Ag strips, loss in metal increases significantly, and thus overall absorption decreases.

We have also calculated overall absorption profiles of the proposed strip-loaded structure when the crystalline silicon active layer is replaced by amorphous silicon or cascaded layers of amorphous silicon and nanocrystalline silicon in the active region. In each case, we have found significant increase in overall absorption in the case of strip-loaded structure when compared with that in planar structure. In particular, in Fig. 6, we show the overall absorption profiles for TM incident light when amorphous silicon is used as the active material instead of crystalline silicon.

### **4.3 Optimized structure**

The fundamental mechanisms behind the absorption enhancement in the proposed structure are the scattering of light by the silicon strips, and therefore, coupling light to photonic modes at the shorter wavelength range, and the excitation of SPPs in the longer wavelength range by the rectangular grooves placed at the silica/metal back contact interface. Therefore, the dimensions of the silicon strips and grooves are critical for light confinement. In Fig. 7, we show the absorption profile in silicon for TM incidence when the silicon strip width varies with fixed dimensions for grooves and when the groove width varies with fixed dimensions for silicon strips. We note that

the resonant wavelengths for photonic and plasmonic modes and the normalized absorption significantly vary when the widths of silicon strips and grooves vary. We optimize the dimensions of the silicon strips and grooves using the particle swarm technique for maximum light absorption. However, we choose optimum values of spacer layer thicknesses, relative position of the silicon strips and grooves in the  $y$ -direction, and periodicity for the silicon strips and grooves from an analysis of parameters sweep. We use an active layer thickness of 300 nm, top and bottom spacer layer thicknesses of 60 nm and 30 nm, respectively, a displacement between the silicon strips and grooves of 80 nm in the  $y$ -direction, and a periodicity for the silicon strips and grooves of 418 nm. Using the particle swarm optimization, we find that the absorption is maximum when the silicon strips have a width of 155.5 nm and the grooves have a width and a depth of 125.7 nm and 50 nm, respectively.

#### **4.4 AM 1.5 solar spectrum weighted absorption**

In the proposed photovoltaic structure, for TM and TE polarized incidence with a flat spectrum ranging from 400 nm–1000 nm, integrated absorption reaches up to 42.8% and 32%, respectively. However, the available solar energy varies with wavelength as shown in Fig. 2. Therefore, for a realistic calculation, the absorption spectra should be weighted by AM 1.5 solar spectrum. Figure 8 shows the absorption spectra weighted by the solar spectrum for both TM and TE polarized incidence. We find that the integrated absorption weighted by AM 1.5 solar spectrum is 34.9% when the incident light is TM polarized and 26.4% when the incident light is TE polarized.

Although we have presented our results for TM and TE incident light, the available solar spectrum at earth's surface can be fairly approximated by 50% contribution from each polarization.

Therefore, we average the solar spectrum weighted absorption spectra for both of the TE and TM polarized incidences and the total solar spectrum weighted integrated absorption becomes 30.7%. Similar calculation for the planar structure without silicon strips and grooves yields an absorption of 21%. However, the inclusion of groove at the back contact of the planar structure yields an absorption of 23.2%. Therefore, the proposed structure, if used instead of planar structure, will offer 45.7% increase in total integrated solar absorption. Figure 9 shows the approximate total solar spectrum weighted absorption spectrum for our optimized structure in comparison with a planar structure without any groove or loading strip. Figure 9 clearly shows that the proposed photovoltaic structure increases light absorption over the entire range of available solar energy.

#### 4.5 Short-circuit current density

For thin photovoltaic structures where the cell thickness is significantly smaller than the diffusion length, all photo-generated carriers can be fairly approximated to be collected at the electrodes [8, 9]. Since the diffusion length of crystalline silicon is on the order of  $\sim 100 \mu\text{m}$ , which is much greater than the 300 nm active region of the proposed structure, we can assume that all photo-generated carriers will be collected at the terminals. Now, if every absorbed photon generates an electron-hole pair, the short-circuit current  $J_{\text{sc}}$  becomes [8]

$$J_{\text{sc}} = q \int_0^{\infty} I(\lambda)R(\lambda)d\lambda, \quad (1)$$

where  $I(\lambda)$  is the solar irradiance,  $R(\lambda)$  is the spectral response of the cell, and  $q$  is the charge of an electron. Using the AM 1.5 solar spectrum weighted absorption given in Fig. 9, we find  $J_{\text{sc}} = 14.4 \text{ mA/cm}^2$  for the proposed silicon strip-loaded plasmonic solar cell.

The  $J_{\text{sc}}$  obtained in the proposed structure is remarkable for a 300 nm crystalline silicon active

layer. As the light confinement increases for an increased transverse dimension of the structure, we find significant increase in  $J_{sc}$  as the active layer thickness increases. We find  $J_{sc} = 19.1 \text{ mA/cm}^2$  when the active layer thickness of the proposed structure is 800 nm without optimized strip width. The  $\sim 43\%$  external quantum efficiency of the  $\sim 300 \text{ nm}$  thick active layer of crystalline silicon of the proposed structure is less than that of state-of-the-art much thicker solar cells [14, 15]. If the active region of the proposed structure is made thicker and the crystalline silicon active layer is replaced by amorphous silicon or nanocrystalline silicon, the quantum efficiency will increase significantly. In particular, in strip-loaded structures with 300 nm amorphous silicon active region and tandem 200 nm amorphous silicon on 100 nm nanocrystalline silicon active region, we have found  $\sim 13\%$  and  $\sim 30\%$  increase of quantum efficiency, respectively, assuming that all the photo-generated carriers are collected at the terminals. Quantum efficiencies of these structures can be increased significantly by optimizing the strip and groove dimensions. By contrast, the quantum efficiency of a solar cell may decrease to some extent due to surface recombination and junction formation at the interfaces.

## 5 Conclusions

In conclusion, the photovoltaic structure that we propose serves the purpose of efficient coupling of incident light to the photonic modes at smaller wavelength region for both TM and TE incidences, as well as to the resonant plasmonic modes at longer wavelength region for TM incidence. The proposed structure exploits a silica layer between the dielectric and metal back contact layer, which considerably reduces the concomitant ohmic loss of plasmonic enhancement. Increased absorption of the available solar energy at the smaller wavelength range for both TM and TE polarizations

is achieved by employing strip-loaded waveguide geometry, which produces field enhancement throughout the solar cell structure at the high absorption spectral regime of silicon. Additionally, the simplicity of the silicon strip-loaded geometry offers an easy fabrication process while leading to greater than 45% increment in total absorption of available solar energy over that obtained in planar silicon solar cell structures.

## **Acknowledgement**

We gratefully acknowledge the support received from the project “Plasmonic photovoltaics for next generation solar cells” funded by Ministry of Education, People’s Republic of Bangladesh at the Department of Electrical and Electronic Engineering of Bangladesh University of Engineering and Technology (BUET) in carrying out this work.

## References

- [1] Stefan A. Maier, *Plasmonics: Fundamentals and Applications* (Springer, 2007).
- [2] D. K. Gramotnev, and Sergey I. Bozhevolnyi, *Nature Photonics* **4**, 83–91 (2010).
- [3] K. Catchpole and A. Polman, *Optics express* **16**, 21793–21800 (2008).
- [4] S. Pillai, K. Catchpole, T. Trupke, and M. A. Green, *Journal of Applied Physics*, **101**, 093105 (2008).
- [5] A. Abass, H. Shen, P. Bienstman, and B. Maes, *Journal of Applied Physics*, **109**, 023111 (2011).
- [6] H. A. Atwater and A. Polman, *Nature materials*, **9**, 205–213 (2010).
- [7] V. E. Ferry, L. A. Sweatlock, D. Pacifici, and H. A. Atwater, *Nano letters* **8**, 4391–4397 (2008).
- [8] V. E. Ferry, Ph.D. Thesis, California Institute of Technology, 2011.
- [9] R. A. Pala, J. White, E. Barnard, J. Liu, and M. L. Brongersma, *Advanced Materials* **21**, 3504–3509 (2009).
- [10] Wen, Long, Fuhe Sun, and Qin Chen., *Applied Physics Letters* **104**, 151106 (2014).
- [11] A. Lin, S. Fu, Y. Chung, S. Lai, and C. Tseng, *Opt. Express*, **21**, A131–A145 (2013).
- [12] L. Zeng, Y. Yi, C. Hong, J. Liu, N. Feng, X. Duan, L. C. Kimerling, and B. A. Alamariu, *Applied Physics Letters* **89**, 111111 (2006).

- [13] P. Bermel, C. Luo, L. Zeng, L. Kimerling, and J. Joannopoulos, *Opt. Express* **15**, 16986–17000 (2007).
- [14] S. Pattnaik, N. Chakravarty, R. Biswas, V. Dalal, and D. Slafer, *Solar Energy Materials and Solar Cells* **129**, 115–123 (2014).
- [15] J. Bhattacharya, N. Chakravarty, S. Pattnaik, W. Dennis Slafer, R. Biswas, and V. Dalal, *Applied Physics Letters* **99**, 131114 (2011).
- [16] R. Biswas, J. Bhattacharya, B. Lewis, N. Chakravarty, and V. Dalal, *Solar Energy Materials and Solar Cells* **94**, 2337–2342 (2010).
- [17] B. Curtin, R. Biswas, and V. Dalal, *Applied physics letters* **95**,231102 (2009).
- [18] S. Pillai, K. R. Catchpole, T. Trupke, and M. A. Green, *Journal of Applied Physics* **101**, 093105 (2007).
- [19] P. Matheu, S. H. Lim, D. Derkacs, C. McPheeters, and E. T. Yu., *Applied Physics Letters* **93**, 113108 (2008).
- [20] V. E. Ferry, Vivian, M. A. Verschuuren, H. B. Li, . E. Schropp, H. A. Atwater, and A. Polman, *Applied Physics Letters* **95**, 183503 (2009).
- [21] M. Verschuuren, and H. V.Sprang, (2007, January), in *MRS Proceedings*, vol. 1002, pp. 1002–N03 (2007).
- [22] V. E. Ferry, J. N. Munday, and H. A. Atwater., *Advanced materials* **22**, 4794–4808 (2010).
- [23] R. G. Hunsperger, *Integrated Optics: Theory and Technology*, (Springer, 2009).

[24] M. Hack, J. McGill, W. Czubyj, R. Singh, M. Shur, and A. Madan, J. Appl. Phys. **53**, 6270 (1982)

[25] S. Okur, M. Gunes, F. Finger, R. Carius, Thin Solid Films **501**, 137 (2006).

[26] A. D. Yaghjian, IEEE Transactions on Antennas and Propagation **55**, 1495–1505 (2007).

## Figure Captions

Figure 1: (a) Schematic diagram of the proposed structure. (b) 2D cross-sectional view of the simulation domain used for finite difference simulation of the proposed structure.

Figure 2: Standard terrestrial solar spectrum irradiance distribution.

Figure 3: Response of the proposed structure to the incident TE and TM polarized light at different wavelengths: (a) Electric field intensity in  $z$ -direction ( $|E_z|^2$ ) for TE incidence at 900 nm, (b) magnetic field intensity in  $z$ -direction ( $|H_z|^2$ ) for TM incidence at 780 nm, (c)  $|E_z|^2$  for TE incidence at 820 nm, and (d)  $|H_z|^2$  for TM incidence at 800 nm.

Figure 4: Absorption spectra in (a) Si and (b) Ag for planar structure, proposed structure with Si strips, and proposed structure with Si strips replaced by Ag strips with TM polarized incidence.

Legends apply for both (a) and (b).

Figure 5: Absorption spectra in (a) Si and (b) Ag for planar structure, proposed structure with Si strips, and proposed structure with Si strips replaced with Ag strips with TE polarized incidence.

Legends apply for both (a) and (b).

Figure 6: Absorption spectra in (a) a-Si and (b) Ag for planar structure and proposed structure with a-Si active region. The incident light is TM polarized. Legends apply for both (a) and (b).

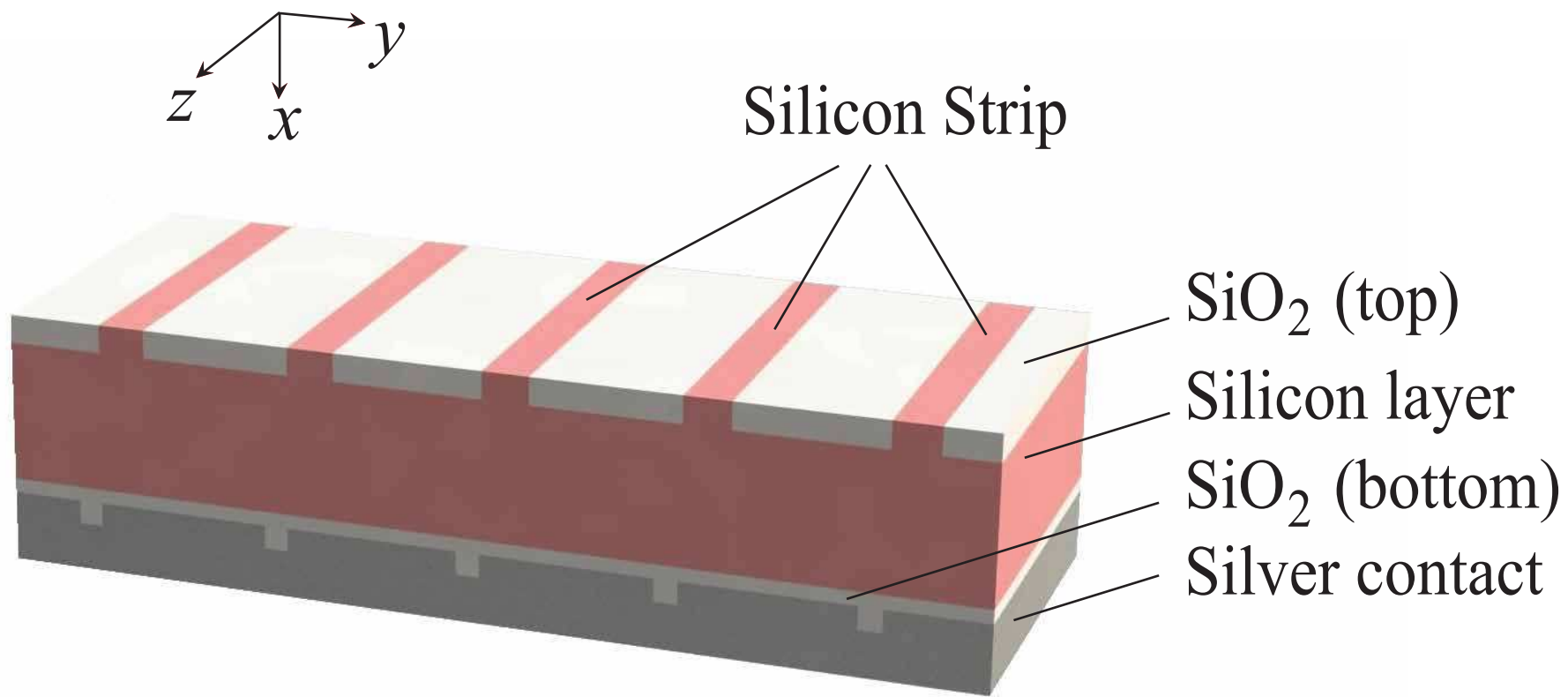
Figure 7: Map of absorption profile in silicon for TM incidence (a) with varying silicon strip width and fixed dimensions for grooves and (b) with varying groove width and fixed dimensions for silicon strips.

Figure 8: Solar spectrum weighted absorption spectra of the optimized structure for TM and TE polarized incidence.

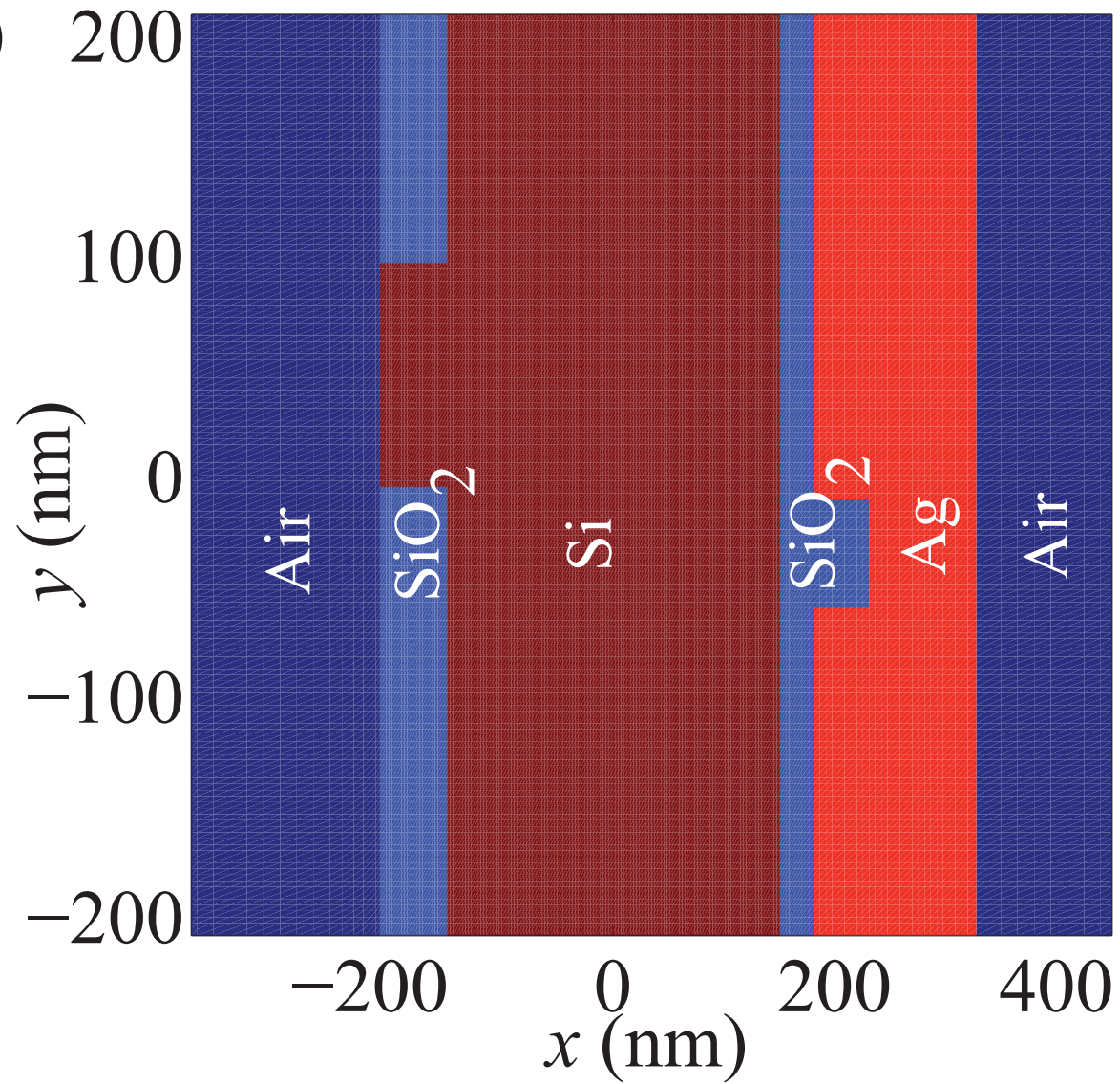
Figure 9: Total solar spectrum (approximated by 50% of each polarization) weighted absorption

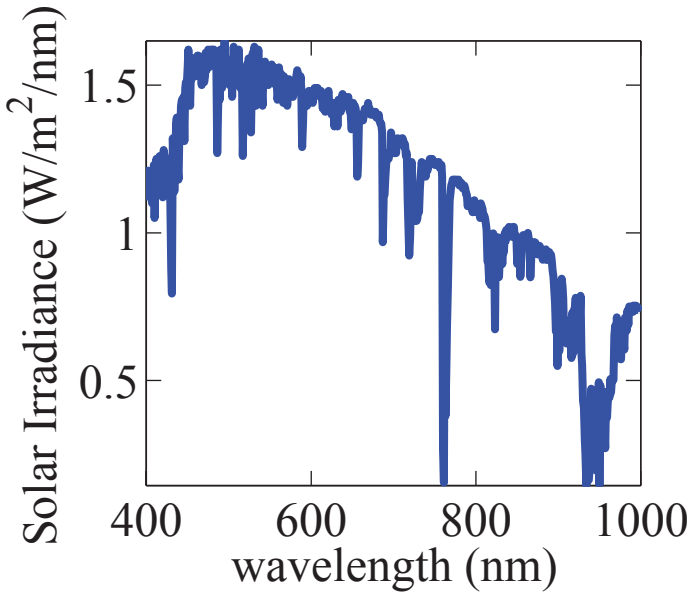
spectra of the optimized structure and a plain structure without grooves at back metal contact and silicon loading strips on the top.

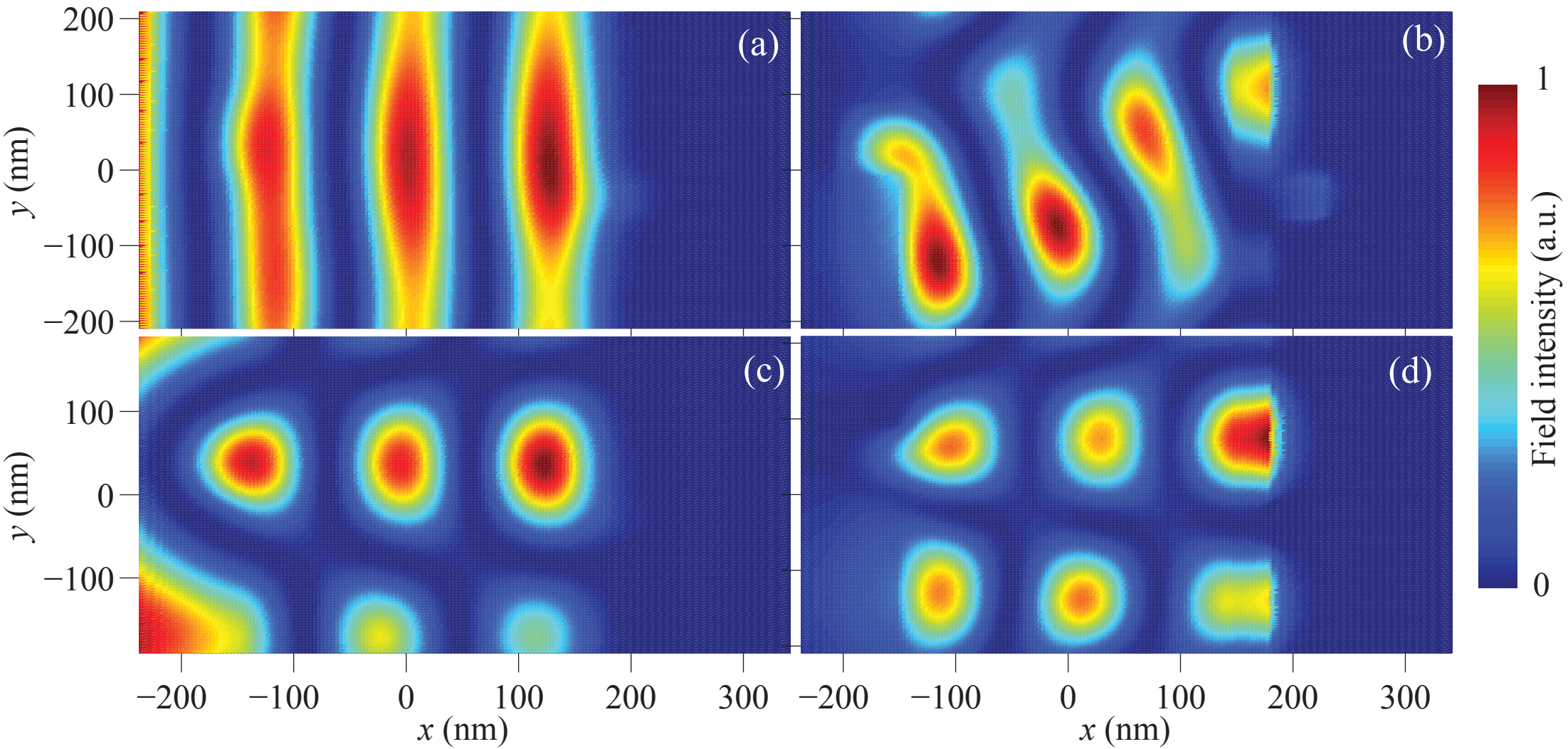
(a)

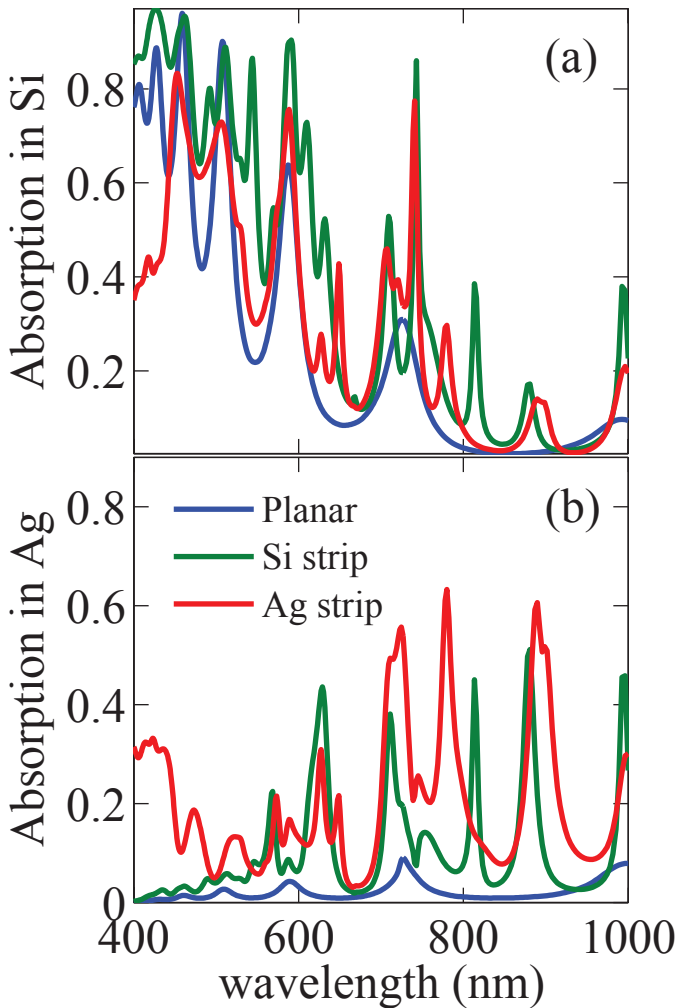


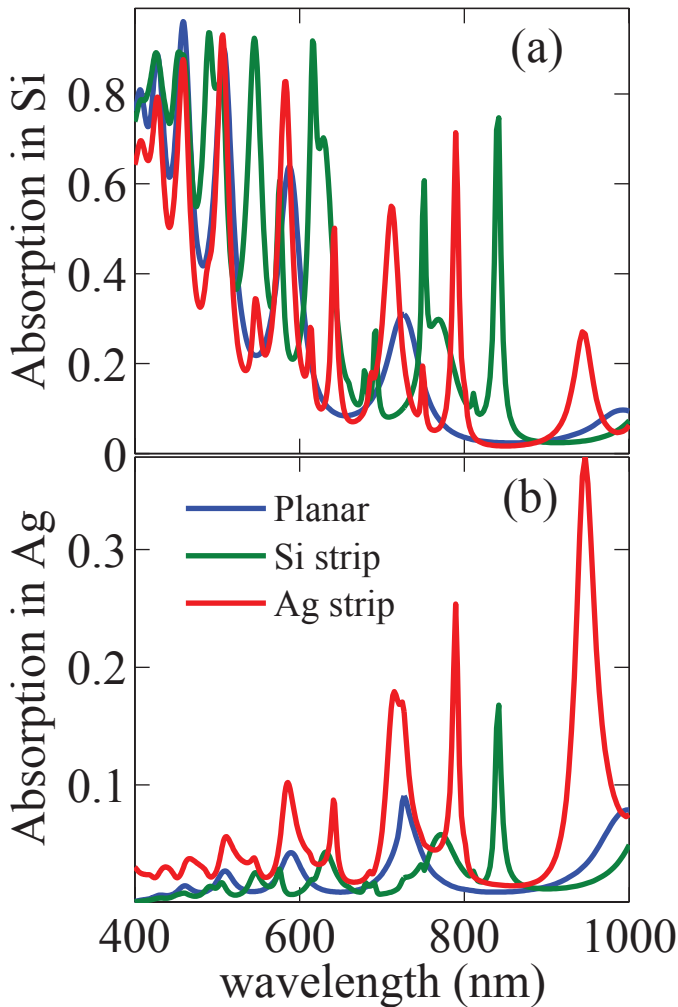
(b)

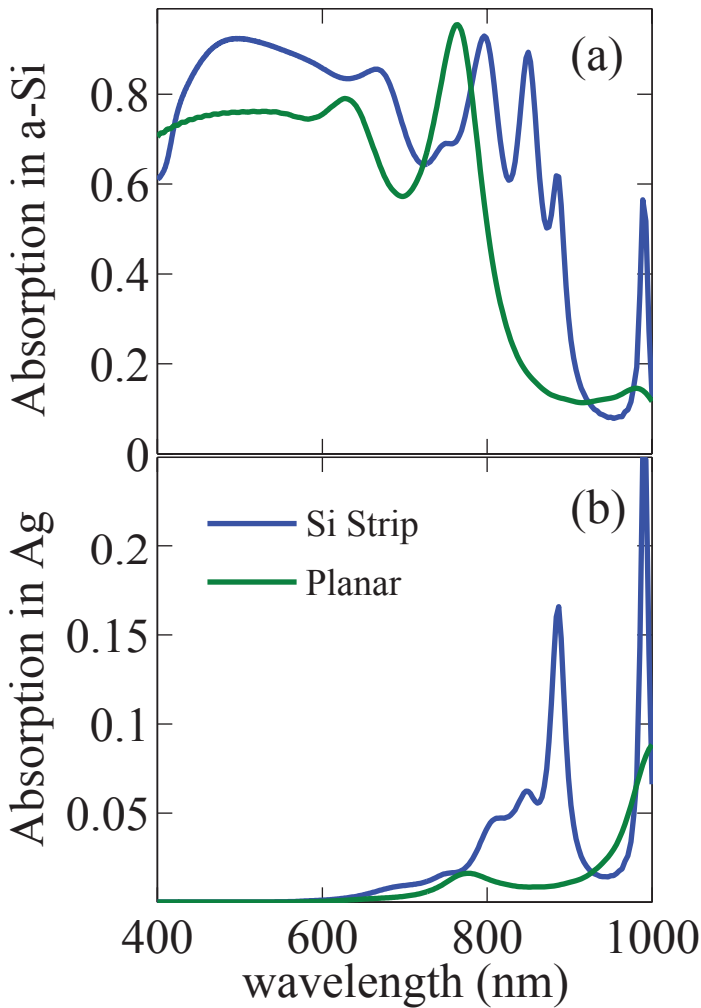


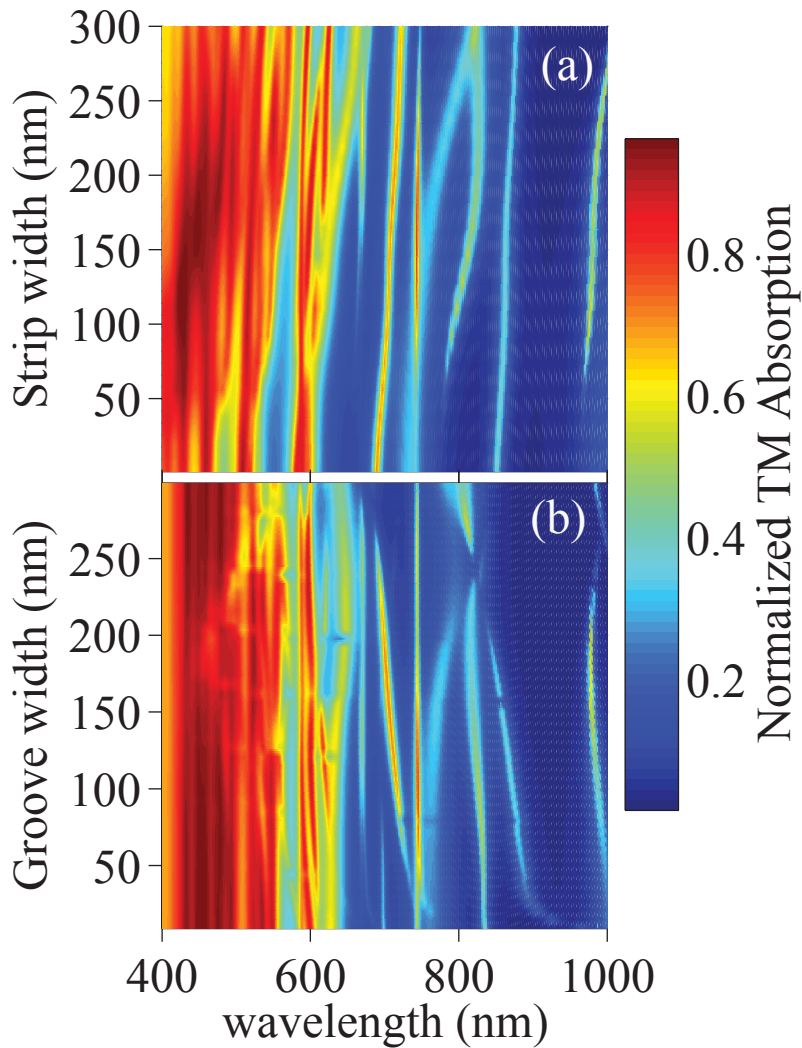












Solar Weighted Absorption

